

Capacitive charging and background processes in carbon nanotube yarn actuators

Tissaphern Mirfakhrai^{a*}, Mikhail Kozlov^b, Mei Zhang^b, Shaoli Fang^b, Ray H Baughman^b
and John D W Madden^a

^aDepartment of Electrical and Computer Engineering and Advanced Materials and Process
Engineering Laboratory, The University of British Columbia,
2332 Main Mall, Vancouver BC, Canada V6T 1Z4

^bNanoTech Institute, The University of Texas at Dallas, Richardson, Texas, 75080

Twist-spun carbon nanotube yarns actuate when extra charge is added to the yarn. This charge can be stored in a double-layer capacitor formed when the yarn is submersed in an electrolyte. The dependence of the actuation stress and strain on the stored charge must be studied if double layer charging models are to be fully verified over large potential ranges. However, background currents are generated in the system when an electrical potential is applied, making it hard to discern the charge stored in the actuator and the charge that passes through the cell due to faradaic processes. A model is developed to separate the capacitive and faradaic portions of the actuator current. The model is then applied to the analysis of the actuation data. The consistency of the results paves the way to understanding the real strain-charge behavior of the actuator.

Keywords: Carbon nanotube actuators, yarns, ionic artificial muscles, modeling, voltammetry

1. INTRODUCTION

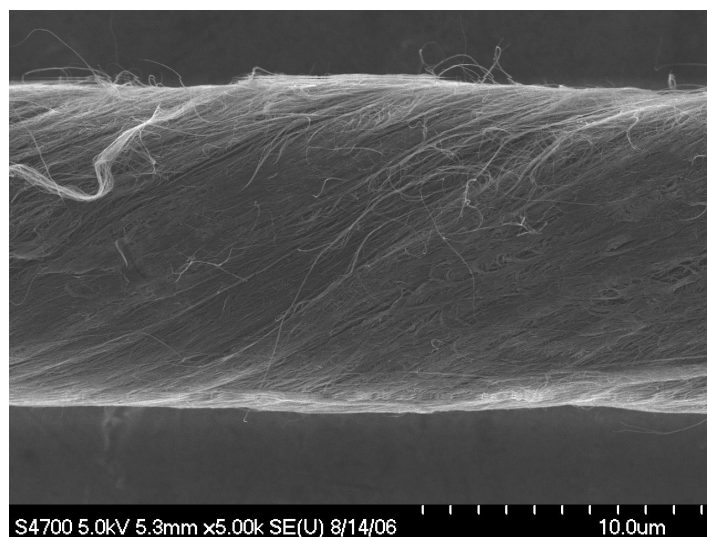


Figure 1: Scanning electron micrograph of twist-spun MWNT yarns

Following on from seminal work demonstrating the electrochemically driven actuation of single walled carbon nanotubes, yarns made through spinning multi-wall carbon nanotubes (MWNTs) [1] have been shown to act as artificial muscles [2]. The CNT yarns used in our experiments are made at the NanoTech Institute of the University of Texas in Dallas, [1]. An MWNT forest is grown on an iron catalyst-coated Si substrate by chemical vapor deposition of acetylene at 680°C. The yarn is started by pulling MWNTs from a side of the nanotube forest. Each nanotube picks up those around it due to van der Waals forces. The spindle and the winding gear are driven by two independent variable-speed

* email: tissa@ece.ubc.ca, Phone: (604) 822-6267

motors allowing for the precise control of twist level. The resulting CNT yarn is shown in Figure 1, similar to those used in the experiments presented in the present article. The yarn imaged here has a diameter of 11.67 μm with a twist angle of about 30°.

We have previously reported the electrochemical actuation of these yarns, which are of particular interest because their tensile strengths and Young's moduli are high and rapidly improving [2], enabling increases in actuator work density and efficiency [1]. They have also been operated as fuel-powered artificial muscles [3, 4]. During electrochemical or fuel cell actuation the yarn is the working electrode (WE) in an electrochemical cell and the presence of an electrolyte is necessary to allow for ion transport required for actuation. The ions that are inserted or removed act to charge or discharge nanotubes within the yarn, and this charging is believed to result in actuation via electrostatic and quantum chemical mechanisms [1]. The electrochemical behavior of the yarns is key to understanding mechanisms and determining performance. In the sections that follow the current and actuation in response to input triangular waves in potential are studied and a method to separate charging and kinetics limited currents demonstrated.

2. MODELING OF THE CAPACITIVE AND PARASITIC CURRENTS

One way of studying the electrochemical behavior of a material is Cyclic Voltammetry (CV). In a CV experiment the current passing through an electrochemical cell, containing the material of interest as the working electrode, is measured while the working electrode potential is swept cyclically over a range. CVs are powerful because substantial information is collected in a short time. However it is often difficult to extract quantitative data from them because of the simultaneous operation of many processes (e.g. mass transport, electron transfer kinetics, double layer charging, solution resistance). We begin with the premise that CNT systems are relatively simple in their electrochemical characteristics, being mostly described by double layer charging reactions and kinetics-limited parasitics (e.g. degradation of the electrolyte). It is expected that the actuation of the yarn is the result of double-layer charging for example [5]. Therefore a pure capacitor, representing the double-layer capacitance, can be considered as a first order approximation for the equivalent circuit for the yarn. Series and parallel resistances and ultimately non-linear elements are added to flesh out this model.

2.1. Double layer Capacitor and leakage resistance

If the potential applied to an ideal capacitor is swept in a cyclic linear fashion, the current versus potential plot is a perfect rectangle spanning the potential range over which the experiment is conducted. However, in general the charge stored in the double-layer may be drained through kinetics or diffusion-limited faradaic reactions, potentially modeled using Butler-Volmer or diffusion-limited behaviors. In this work, it is assumed that the experiments are conducted in clean environments such that currents due to Nernstian reactions are negligible. For now, let us assume that the potential drop across the yarn electrode is sufficiently small such that the leakage due to the reactions can be modeled by a resistor R_p , itself a function of the working electrode (WE) potential, V . If a resistor is included in parallel with the capacitor to represent leakage, the original rectangular CV will be tilted into a parallelogram with a tilt angle that is a function of the resistance of the leakage resistor. Figure 2a shows the calculated CV for a pure capacitor and a parallel R-C circuit.

The experimental CV of the CNT yarn actuator in its middle potential range Figure 2c) resembles the parallelogram in Figure 2a, suggesting that it too may be viewed as a superposition of capacitive and leakage currents. We therefore propose to break down the total measured cell current i_T as:

$$i_T = i_C + i_p.$$

The current i_C is the capacitive part of the current and can be expressed as $i_C = C \frac{dV}{dt}$, where V is the working electrode potential versus the reference. The current i_p is the leakage current flowing through the resistor and for now we assume it to be only a function of the working electrode potential, i.e. $i_p = f(V)$, which is expected in a kinetics-limited parasitic reaction but not for mass transport limited cases. Assuming this model the cell current i_T can be expressed as:

$$i_T = C \frac{dV}{dt} + f(V).$$

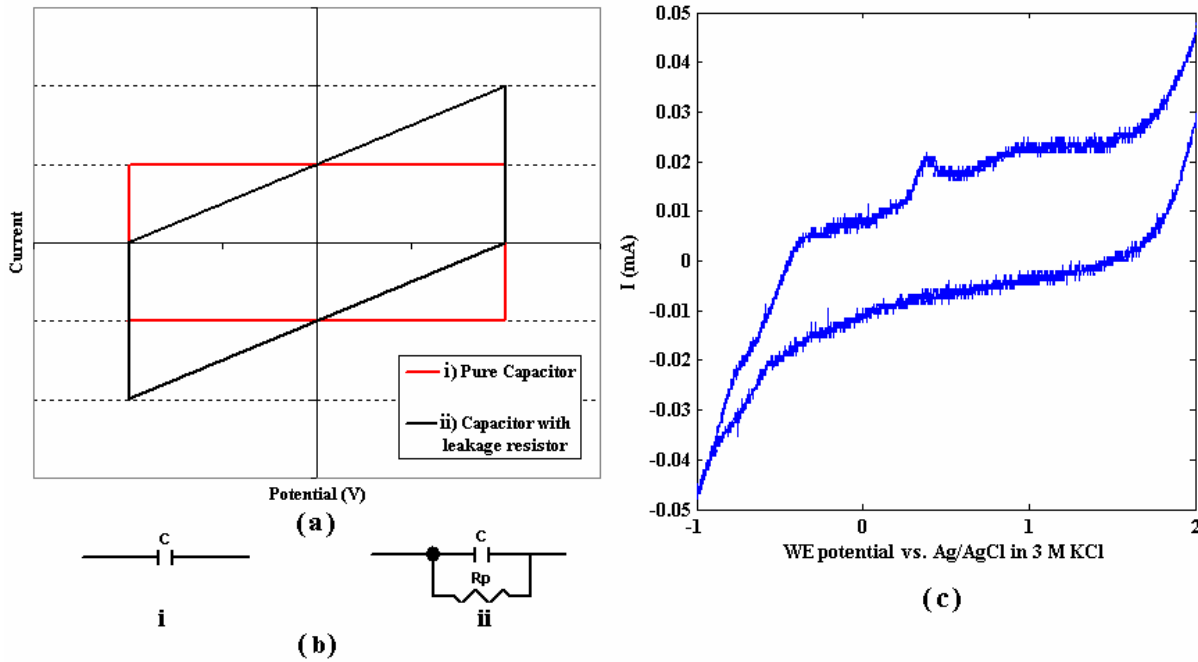


Figure 2: (a) The cyclic voltammogram for the circuits drawn in (b) i. pure capacitor and ii. parallel combination of a capacitor and a resistor and (c) cyclic voltammogram for the CNT yarn actuator in an electrolyte made of 0.2 M tetrabutylammonium hexafluorophosphate in acetonitrile, viewed over a potential for comparison

When the WE potential sweep is in the positive direction, $\frac{dV}{dt} = +\alpha$, where α is the CV scan rate. So

$i_T^+ = +\alpha C + f(V)$. During the potential sweep in the negative direction, $\frac{dV}{dt} = -\alpha$ and so

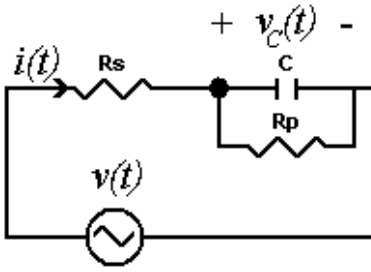
$i_T^- = -\alpha C + f(V)$. Therefore: $i_T^+ + i_T^- = 2f(V)$ and $i_T^+ - i_T^- = 2\alpha C$. The capacitance and the leakage current can be estimated as a function of the current by:

$$C = \frac{i_T^+ - i_T^-}{2\alpha}, \quad f(V) = \frac{i_T^+ + i_T^-}{2}.$$

The current is thus divided between a capacitive part proportional to the scan-rate and a rate-independent current $f(V)$. The accuracy of the model depends on this condition being satisfied and we shall test for it later.

2.2. Parallel and series RC model

In most cases, unless the electrodes are close to each other, the resistance of the solution and the contacts cannot be neglected. Therefore we need to introduce a resistance in series with the above parallel RC to model these resistances. When a series resistance is included to account for the solution and contact resistances, matters become more complicated. The differential equations governing the system are now:

$$\begin{cases} i(t) = C \frac{dv_c(t)}{dt} + \frac{v_c(t)}{R_p} \\ v(t) = v_c(t) + R_s i(t) \end{cases}$$


Solving for $i(t)$:

$$i(t) = \frac{v(t) - v_c(0)e^{\frac{-t}{RC}}}{R_s} - \frac{e^{\frac{-t}{RC}}}{R_s^2 C} \int_{\tau=0}^t v(\tau) e^{\frac{\tau}{RC}} d\tau$$

During the rising cycle of a CV, $v(t) = V_L + \alpha t$, where V_L is the lower bound of the potential at which we start the cycle and α is the scan rate. Substituting in the above equation we obtain

$$i_+(t) = \frac{V_L + \alpha t - v_c(0)e^{\frac{-t}{RC}}}{R_s} - \frac{e^{\frac{-t}{RC}}}{R_s^2 C} \int_{\tau=0}^t (V_L + \alpha \tau) e^{\frac{\tau}{RC}} d\tau$$

where $R = R_s \parallel R_p = \frac{R_s R_p}{R_s + R_p}$. After calculating the integral:

$$i_+(t) = \frac{V_L + \alpha t}{R_s} - \frac{R}{R_s^2} (V_L + \alpha t) + \frac{\alpha C R^2}{R_s^2} + \frac{e^{\frac{-t}{RC}}}{R_s} (-v_c(0) + \frac{R V_L}{R_s^2} - \frac{\alpha C R^2}{R_s^2})$$

If $t_+ \gg RC$, i.e. the time passed is considerably longer than the system's time constant (or the scan rate is very slow

and we are away from the turning points of the CV), the terms including $e^{\frac{-t}{RC}}$ become negligibly small and the above result can be simplified to

$$i_+(t) = \frac{V_L + \alpha t}{R_s + R_p} + \frac{\alpha R^2 C}{R_s^2}$$

Similarly, during the down-sweep of a CV, (i.e. $t > T$), $v(t) = V_H - \alpha(t - T)$, where V_H is the upper bound of the potential during the CV and T is the point of time when the potential has reached V_H and is beginning to decrease.

$$i_-(t) = \frac{V_H - \alpha(t - T) - v_c(0)e^{\frac{T-t}{RC}}}{R_s} - \frac{e^{\frac{-t}{RC}}}{R_s^2 C} \int_{\tau=0}^t (V_0 - \alpha(\tau - T)) e^{\frac{\tau}{RC}} d\tau$$

where $R = R_s \parallel R_p = \frac{R_s R_p}{R_s + R_p}$. After integration:

$$i_-(t) = \frac{V_H - \alpha(t - T) - v_c(0)e^{-\frac{t-T}{RC}}}{R_s} - \frac{R}{R_s^2}(V_H - \alpha(t - T) + \alpha RC) - \frac{R}{R_s^2}e^{-\frac{t}{RC}}(V_L(e^{\frac{T}{RC}} - 1) - V_H e^{\frac{T}{RC}} + \alpha T e^{\frac{T}{RC}} + 2\alpha RC(1 - e^{\frac{T}{RC}}))$$

If $t_- > T \gg RC$, i.e. during the down-sweep and assuming that the time passed before switching the sweep direction is considerably longer than the system's time constant, the above result can be simplified to

$$i_-(t) = \frac{V_H - \alpha(t - T)}{R_s + R_p} - \frac{\alpha R^2 C}{R_s^2}$$

So far we have found that:

$$\begin{cases} i_+(t) = \frac{V_L + \alpha t}{R_s + R_p} + \frac{\alpha R^2 C}{R_s^2} & t \leq T \\ i_-(t) = \frac{V_H - \alpha(t - T)}{R_s + R_p} - \frac{\alpha R^2 C}{R_s^2} & t > T \end{cases} \Rightarrow \begin{cases} i_+(t_+) = \frac{V_+}{R_s + R_p} + \frac{\alpha R^2 C}{R_s^2} \\ i_-(t_-) = \frac{V_-}{R_s + R_p} - \frac{\alpha R^2 C}{R_s^2} \end{cases}$$

where $V_+ = V_L + \alpha t_+$ and $V_- = V_H - \alpha(t_- - T)$ and t_+, t_- are the times during one cycle at which the potential reaches V_+, V_- respectively. Looking at the currents i_+ and i_- at a given potential, $V_+ = V_- = V$ and we can say that

$$\frac{i_+ + i_-}{2} = \frac{V_+ + V_-}{2(R_s + R_p)} + \frac{\alpha R^2 S}{R_s^2} - \frac{\alpha R^2 S}{R_s^2} = \frac{V}{R_s + R_p}$$

which is only a function of the potential at that point V . Therefore we call it $f(V)$:

$$\Rightarrow f(V) = \frac{V}{R_s + R_p} \quad (1)$$

If $R_p \gg R_s$, then $\Rightarrow f(V) \cong \frac{V}{R_p}$, i.e. the slope of $f(V)$ versus V is $\frac{1}{R_p}$ and R_p can be determined by

measuring that slope. The capacitive current is given by:

$$\begin{aligned} i_{cap} &= \frac{i_+|_V - i_-|_V}{2} = \frac{(\frac{V_+}{R_s + R_p} + \frac{\alpha R^2 C}{R_s^2}) - (\frac{V_-}{R_s + R_p} - \frac{\alpha R^2 C}{R_s^2})}{2} \\ &= \frac{\frac{V}{R_s + R_p} - \frac{V}{R_s + R_p} + \frac{2\alpha R^2 C}{R_s^2}}{2} = \frac{\alpha R^2 C}{R_s^2} \end{aligned}$$

$$\Rightarrow i_{cap} = \frac{\alpha R^2 C}{R_s^2} = \frac{\alpha R_s^2 R_p^2 C}{R_s^2 (R_s + R_p)^2} = \frac{\alpha C}{(1 + \frac{R_s}{R_p})^2}$$

If $R_p \gg R_s$ then

$$\Rightarrow i_{cap} \cong \alpha C \Rightarrow C = \frac{i_{cap}}{\alpha} \quad (2)$$

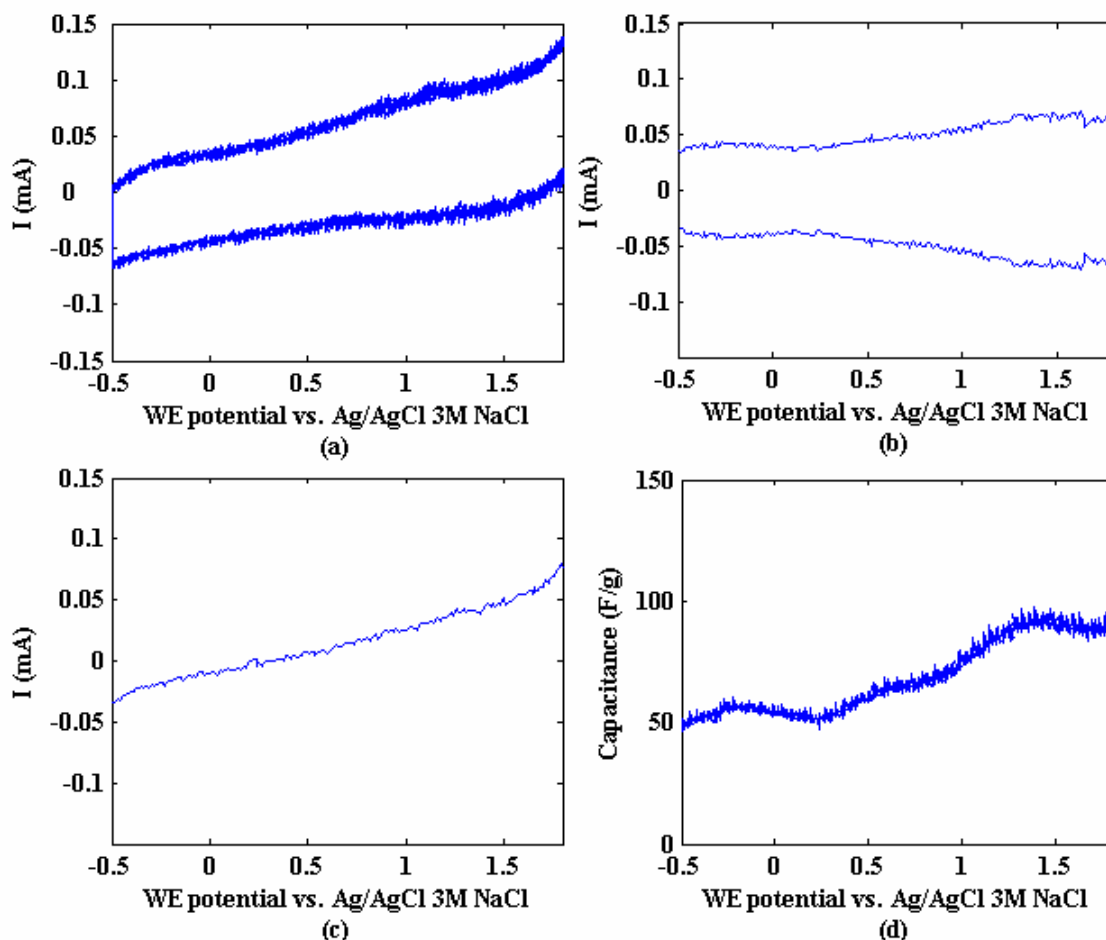


Figure 3: (a) The cyclic voltammogram for the CNT yarn actuator in an electrolyte made of 0.2 M tetrabutylammonium hexafluorophosphate in acetonitrile viewed over a potential range of -0.5 to 1.8 V (b) the capacitive part (c) the leakage background current and (d) the gravimetric capacitance as computed using the capacitive current in (b)

Figure 3a shows the experimental CV for the actuation of CNT yarn with a diameter of 18 μm during a CV in a 0.2 M solution of tetrabutylammonium hexafluorophosphate (TBAP) in acetonitrile under a constant 20 MPa of stress. The counter electrode was a piece of carbon fibre paper (Ballard AvCarb P-50T). The same counter electrode has been used for all experiments in this paper. The respective capacitive and leakage currents computed using the $R_s - R_p - C$ model (equations 1 and 2) are plotted Figure 3b and c as a function of the working electrode potential. The capacitance as a function of potential, calculated for this sample based on the above method is plotted in Figure 3d. $R_s + R_p$ is

estimated from the slope of the line in Figure 3b to be about $48 \text{ k}\Omega$ s. R_s is measured to be approximately $1.5 \text{ k}\Omega$ by studying the step response of the system. Thus the condition that $R_p \gg R_s$ seems to have been satisfied. C_g at $V=0 \text{ V}$ is estimated to be $55 \pm 1.5 \text{ F/g}$.

2.3. Kinetics-limited parasitic reactions and diode model

Beyond certain potentials in both positive and negative directions the magnitudes and contributions of these component currents seem to change as a function of the applied WE potential. This can be seen from the irregular shape of the CV in Figure 4a, which is exactly the same as those in Figure 3 except viewed over a larger potential range.

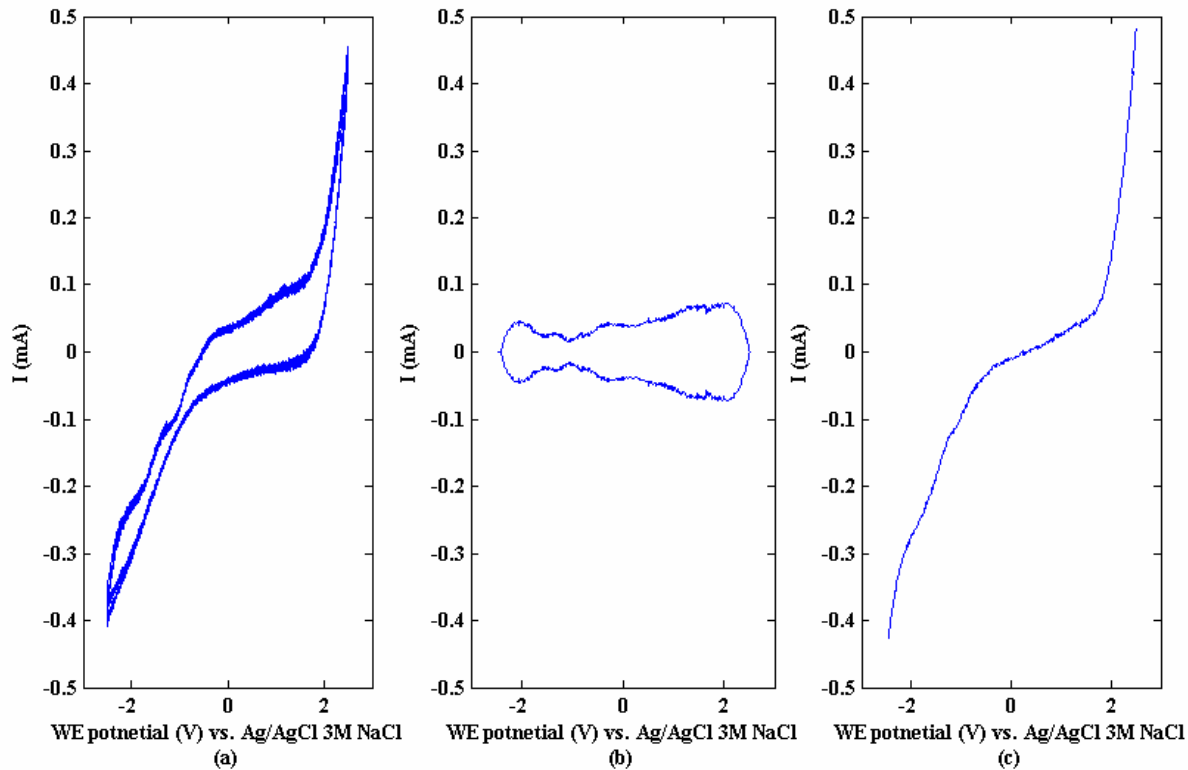


Figure 4: (a) The cyclic voltammogram for the CNT yarn actuator in an electrolyte made of 0.2 M tetrabutylammonium hexafluorophosphate in acetonitrile, viewed over a potential range of -2.5 to 2.5 V versus reference (b) the capacitive part and (c) the leakage background current

As can be seen from Figure 4c, there is a significant and abrupt rise in the parasitic current below -1 V and above +1.5 V. This suggests that the reaction modeled by R_p might best be modeled using a non-linear relationship such as the Butler-Volmer equation [6]. With this assumption the governing differential equations for the circuit in Figure 5a will be

$$V(t) = v_c(t) + i_{bv} R_s + R_s C \frac{dv_c}{dt} \text{ resulting in}$$

$$\frac{d\eta}{dt} + \frac{\eta}{R_s C} + \frac{i_0}{C} (e^{(1-\beta)f\eta} - e^{-\beta f\eta}) = \frac{V(t) - E_0}{R_s C} \quad (3).$$

Here R_s and C are defined as before, η is the overpotential across the electrode, β is the transfer coefficient, $f = F/RT$ (where F is Faraday's constant, R is the molar gas constant and T is the absolute temperature) and E_0 is the

standard potential of the reaction considered. The three terms to the left of equation (3) behave as a capacitance, a resistance and two diodes ($i = i_0 e^{\frac{nV}{RT}}$ behavior) respectively in terms of equivalent circuit elements. The difference in the signs of the two exponential terms indicates that the two diodes must be mounted in opposite directions to model the reaction in the forward and the reverse directions. Therefore we propose to model the system with the circuit in Figure 5b. In general, there may be more than one reaction happening in either positive or negative potentials, therefore more than one diode branch may exist in parallel in each direction to model different reactions. Figure 6a shows the model with parameters calculated for the CV in Figure 4a. Circuit simulation results using *Electronics Workbench 5.12* and the experimental CV are in close agreement (Figure 6b). The CV fits nicely with one assuming a capacitance of $180 \mu\text{F}$ (equivalent of 55 F/g , the capacitance at 0 V) parallel with a Butler-Volmer branch with standard potential of 1.9 V versus reference and $i_0 = 1.5 \mu\text{A}$. R_s is again found to be around $1.5 \text{ k}\Omega$.

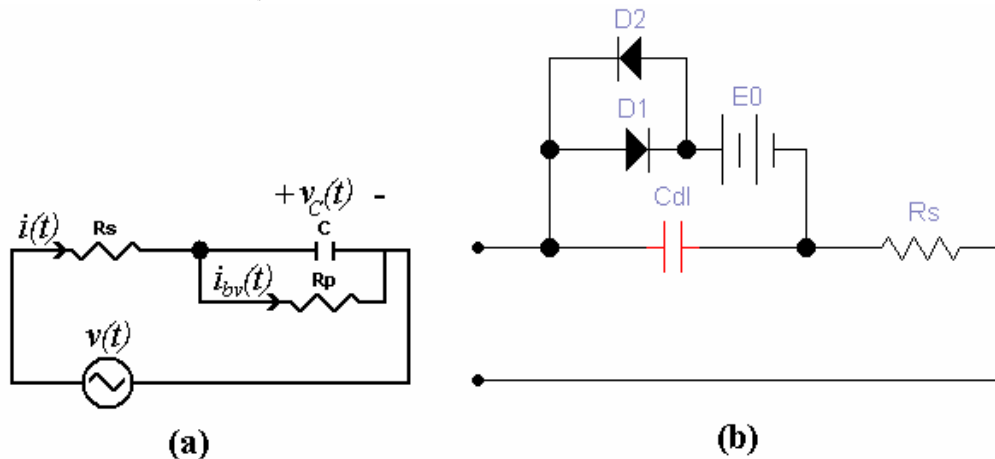


Figure 5: (a) Equivalent circuit with potential-dependent R_p to model for parasitic reactions and (b) equivalent circuit model for the CNT yarn electrode in the cell, accounting for capacitance, solution and series resistance, leakage and Butler-Volmer type reactions

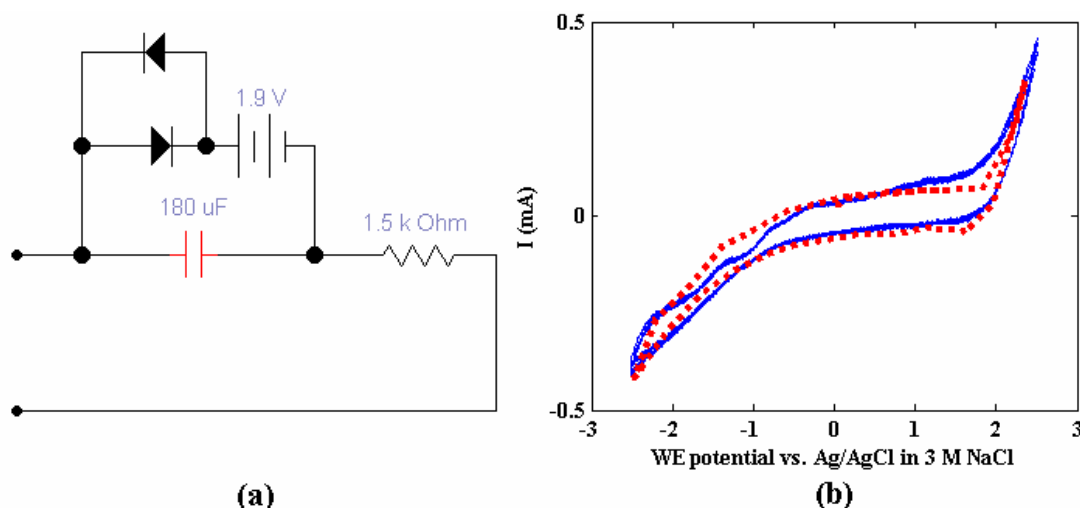


Figure 6: (a) The circuit model for the system studied in Figure 4 and (b) the comparison of the simulation results from the model and the experimental CV

3. DISCUSSION

In order for the model to be accurate, it is important to prove that the parasitic current $f(V)$ does not depend on the scan rate. The model was applied to the experimental data for the same sample at scan rates of 100 and 250 mV/s . The

computed parasitic currents are plotted in Figure 7. As can be seen, even though the scan rate is 2.5 times larger, the computed parasitic currents are virtually the same. This will be the case as long as currents from diffusion-limited faradaic processes are negligible. Currents from diffusion-limited processes such as those due to contamination are neither independent of rate nor proportional to it (e.g. they could be proportional to the square root of the rate). Therefore the assumptions of our model will no longer be satisfied and the accuracy of the model decreases. In such cases part of the current due to faradaic processes will erroneously appear in both computed capacitive and parasitic currents unless the corresponding peaks in the original CV are detected and removed before computing i_{cap} and $f(V)$. It is also evident from Figure 7 that the slopes of the two kinetics-limited tails of the plot are different in the positive and negative directions. This implies either the existence of multiple reactions in different directions or a kinetics-limited reaction that flows more easily in one direction than the other. Preliminary analysis of the data from the fitting predicts that the capacitance may depend on the scan rate of the CV. The change in capacitance in response to a 100-fold change in the scan rate in an aqueous electrolyte is estimated at about 30 %, closer to those measured for porous carbon electrodes by Oren and Soffer for in [7] than those measured for carbon single-walled nanotubes in [8].

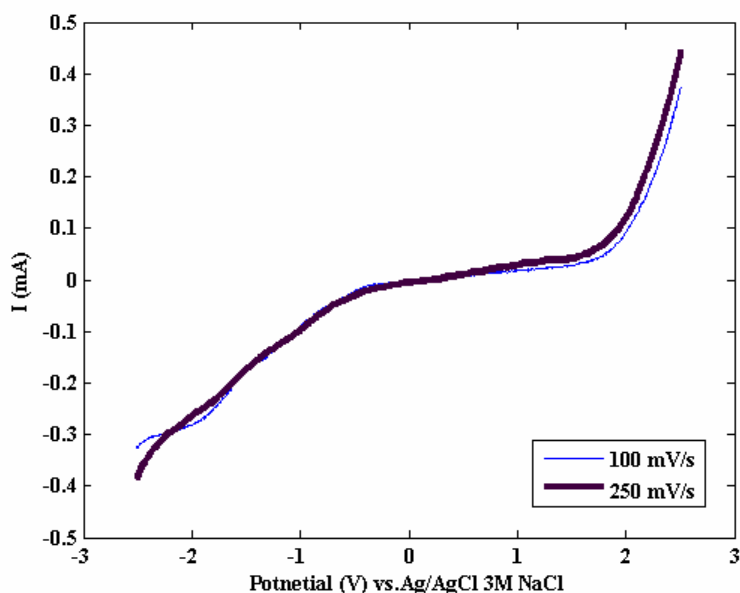


Figure 7: Comparison of the calculated $f(V)$ parasitic current for the same CNT yarn sample as above at 100 mV/s (thin) and 250 mV/s (bold)

As an example for the application of the model, let us consider the strain response of the CNT yarn actuator to a cyclic voltammogram. A general relationship is expected to exist between the actuation strain and the charge stored in the actuator. If the actuator charge is taken as the integral of the total cell current, the charge contributing to parasitic reactions will be included. Such parasitic reactions are especially problematic at very positive or very negative potentials, where the currents due to those reactions increase almost exponentially. The model promises to allow the separation of these components.

Figure 8 shows the strain in response to the potentials and currents shown in Figure 3. The strain (compensated for creep by subtracting a line) and the total charge are plotted in (a) and (b) versus time. The origin of the charge axis is arbitrary as we don't know the initial charge of the yarn. In Figure 8c the strain in (a) is plotted versus the total charge in (b). The resulting plot is confusing and it is hard to extract any information about the relationship between strain and charge out of it. The model is now applied to the CV for this experiment (Figure 3a) by dividing the current into the rate-independent $f(V)$ (Figure 3c) and the capacitive current i_{cap} (Figure 3b). The stored charge is calculated by integrating the capacitive current.

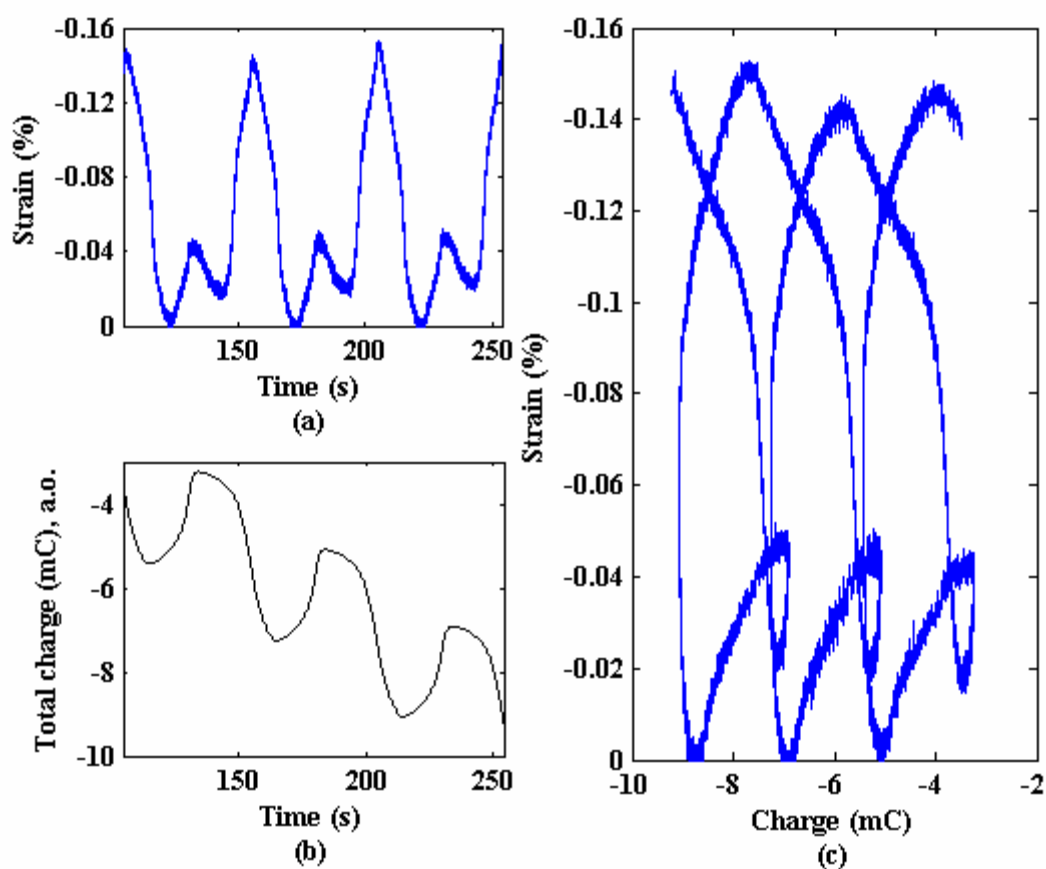


Figure 8: (a) Strain (compensated for creep) vs. time (b) total charge vs. time (vertical axis origin arbitrary) and (c) strain in (a) vs. charge in (b), during a CV of the CNT yarn in a 0.2 M solution of TBAP in acetonitrile under a 20 MPa of load

Figure 9a shows the same strain as in Figure 8a. Figure 9b shows the stored charge versus time as found by integrating the capacitive part of the current in Figure 3b. The strain and the stored charge are plotted versus each other in Figure 9c. This plot is comparable with the results reported in [9] for carbon single-walled nanotubes. The dotted red line shows a quadratic fit. The hysteric effect may be due to the charge consumed in diffusion-limited reactions that had been counted as part of the capacitive current and other anomalies in the CVs due to effects other than capacitance or butler-volmer type reactions or to the nonlinear nature of the creep which has been assumed to be linear. Some reactions running due to contaminations at the electrodes seem to contribute to the current in the shape of some Nernstian peaks (e.g. the small peak in Figure 4a around -1 V). This means that if such peaks were accounted for before computing i_{cap} and $f(V)$, the stored charge profile in Figure 9b would probably exhibit an asymmetric behavior corresponding to the asymmetric behavior of the strain profile in Figure 9a. Under such circumstances the strain-charge plot of Figure 9c is expected to retrace itself without the hysteresis. The presence of impurities (redox mediators) in the electrolyte that act to shuttle charge between electrodes can dissipate charge under open-circuit conditions. Also, faradaic processes occurring at only one electrode can result in differences in the amount of capacitively-stored charge in the two electrodes. Further study and modeling is needed in order to diagnose the nature of the anomalies in the CV to obtain the true relationship between the strain and the stored charge.

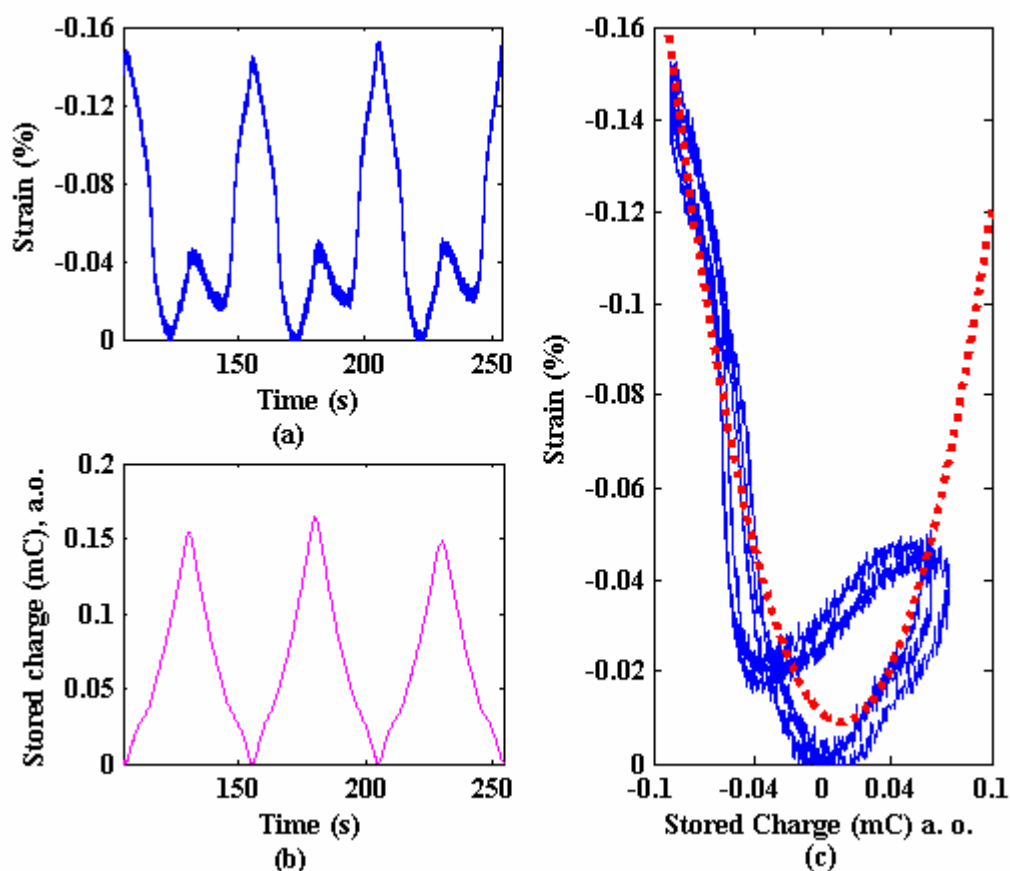


Figure 9: (a) Strain (compensated for creep) vs. time (b) stored charge vs. time (vertical axis origin arbitrary) and (c) strain in (a) vs. charge in (b), during a CV of the CNT yarn in a 0.2 M solution of TBAP in acetonitrile under a 20 MPa of load. The parabola in (c) shows a quadratic fit.

4. CONCLUSIONS

A circuit model is presented to model the electrochemical behavior of a carbon nanotube yarn actuator. This model simplifies the computation of the capacitance and leakage resistances of the yarn and paves the way for a better understating of the strain-charge relationship in ionic artificial muscles especially yarns and actuators made of carbon nanotubes.

REFERENCES

1. Zhang, M., K.R. Atkinson, and R.H. Baughman, *Multifunctional carbon nanotube yarns by downsizing an ancient technology*. Science, 2004. 306(5700): p. 1358-1361.
2. Mirfakhrai, T., et al., *Electrochemical actuation of carbon nanotube yarns*. Smart Materials and Structures, 2007. 16(2).
3. Kozlov, M., et al. *From electrical to fuel-powered artificial muscles*, in *EAPAD: Smart Structures and Materials 2007: Electroactive Polymer Q.3 Actuators and Devices*; . 2007. San Diego, CA: SPIE.
4. Ebron, V.H., et al., *Fuel-powered artificial muscles*. Science, 2006. 311(5767): p. 1580-1583.
5. Baughman, R.H., et al., *Carbon nanotube actuators*. Science, 1999. 284(5418): p. 1340-1344.
6. Bard, A.J. and L.R. Faulkner, *Electrochemical Methods, Fundamentals and Application*. 2nd ed. 2001, New York: Wiley.

7. Oren, Y. and A. Soffer, *The electrical double layer of carbon and graphite electrodes. Part II. Fast and slow charging processes*. Journal of Electroanalytical Chemistry, 1985. 186: p. 63-77.
8. Barisci, J.N., G.G. Wallace, and R.H. Baughman, *Electrochemical studies of single-wall carbon nanotubes in aqueous solutions*. Electrochemistry Communications, 2000. 488: p. 92-98.
9. Spinks, G.M., et al., *Carbon Nanotube Actuators: Synthesis, Properties, and Performance*, in *Electroactive Polymers (EAP) Actuators as Artificial Muscles, Reality, Potential and Challenges* Y. Bar-Cohen, Editor. 2004 SPIE press: Bellingham WA. p. 261-95.